FORUM GEOGRAFI
ISSN: 0852-0682 | E-ISSN: 2460-3945
HTTPS://JOURNALS.UMS.AC.ID/INDEX.PHP/FG/

Research article

Analysis and Geovisualization of Tsunami Hazard and Evacuation Routes in the Opak-Progo Coastal Area

Sudaryatno Sudaryatno[1,*], Josaphat Tetuko Sri Sumantyo[2], Taufik Hery Purwanto[1], Muhammad Falakh Al Akbar[1], Amelia Rizki Gita[1], Osmar Shalih[3]

[1] Department of Geographic Information Science, Faculty of Geography, Universitas Gadjah Mada, Yogyakarta.
[2] Center for Environmental Remote Sensing, Chiba University, Yayoi-Cho, Inage-Ku, Chiba-Shi, Japan.
[3] Badan Nasional Penanggulangan Bencana/BNPB-RI, Jakarta, Indonesia.

[*)] Correspondence: sudaryatno@ugm.ac.id

Citation:
Sudaryatno, S., Sumantyo, J. T. S., Purwanto, T. H., Akbar, M. F. A., Gita, A. R., & Shalih, O. (2024). Analysis and Geovisualization of Tsunami Hazard and Evacuation Routes in the Opak-Progo Coastal Area. Forum Geografi. 38(2), 257-265.

Article history:
Received: 13 June 2024
Revised: 8 August 2024
Accepted: 20 August 2024
Published: 27 August 2024

Abstract

The southern coastal area of Java has a high risk of tsunamis. Additionally, the presence of rivers flowing in the south of Java Island poses a greater tsunami threat because these rivers can act as "toll roads" for tsunami waves to enter the land. Therefore, this study was conducted in the coastal area of the Opak-Progo watershed to determine the level of tsunami hazards and plan effective evacuation routes. The hazard map was created using the Berryman method, which employs parameters such as slope, surface roughness coefficient, coastline, and tsunami run-up height scenario; a 3-metre scenario was used in this study. Network analysts also determined evacuation routes using the nearest facility method. Network analysis was used to identify an optimised route with four evacuation sites. This research has the potential to significantly contribute to tsunami mitigation and evacuation planning in the coastal areas of the Opak-Progo watershed.

Keywords: Berryman; Tsunami hazard level; Network Analyst; Tsunami evacuation route.

1. Introduction

Indonesia is a disaster-prone country (BNPB, 2023; Herlianto, 2023) due to its location at the confluence of three tectonic plates: the Indo-Australian Plate, the Eurasian Plate, and the Pacific Plate (Friska *et al.*, 2022). This confluence has made Indonesia vulnerable to tectonic and volcanic activity (Hartoko *et al.*, 2016; Muttaqy *et al.*, 2022; Sinaga & Ronoatmojo, 2022). Tectonic and volcanic activities are among the causes of tsunamis (Sugawara, 2020), alongside underwater or coastal landslides and falling celestial bodies (Wang *et al.*, 2022; Zorn *et al.*, 2022). The term “tsunami” describes a very large ocean wave generated by a vertical change in water mass, associated with a sudden influx of water in the sea (Katsumata *et al.*, 2021; Richard *et al.*, 2023). Although tsunamis occur less frequently than other natural disasters, they can cause significant-damage (Amalia Listiani & Fuji Lestari, 2023; Srinivasa Kumar *et al.*, 2023). According to the catalogue of Indonesian tsunamis from 416 to 2018 released by the Earthquake and Tsunami Centre of the Department of Geophysics, Meteorology, and Climatology (BMKG) in 2019, there have been 188 recorded tsunamis of varying heights.

Seismic gap zones can trigger megathrust earthquakes of greater magnitude (Ehara *et al.*, 2023; Sudaryatno *et al.*, 2022). The seismic gap zone south of Java lies between the southern Java Coast and the Java trench. It exhibits weak seismicity but intense slip deficits, making it a potential source of future megathrust earthquakes (Rusydi & Masitoh, 2023; Ry *et al.*, 2023). The littoral zone of Java Island, particularly in the Special Region of Yogyakarta, could be affected by a 20-metre tsunami (Widiyantoro *et al.*, 2020). If such an event occurs, the coast of Yogyakarta will experience enormous damage due to the absence of barrier islands and a lack of damping vegetation in the area (Tarigan *et al.*, 2015).

The presence of river mouths in a watershed can also exacerbate inundation during tsunami disasters (Adityawan & Tanaka, 2016; Fuad *et al.*, 2022). This research aims to map the geovisualisation of tsunami hazards in the littoral region of the Opak and Progo watersheds. A watershed integrates a river and its tributaries, functioning naturally to hold, retain, and drain water from rainfall to the lake or sea (Ovando, 2023). Watersheds flowing directly into the ocean are particularly threatened when tsunami waves arrive (Liu *et al.*, 2022; Tanaka & Tinh, 2022). This is because the waterways can serve as "toll roads" for tsunami waves, facilitating water overflow onto land and increasing the extent of inundation. Tsunami disasters can be unpredictable; thus, disaster management is essential to mitigate their impacts and potential damage (Andriani *et al.*, 2023; Kirana & Bature, 2022; Shalih *et al.*, 2020). One possible action is non-structural mitigation on through the provision of tsunami hazard maps (Bai *et al.*, 2023; Bosma *et al.*, 2023; Zelaya *et al.*, 2023). Hazard maps can be created using remote sensing technology (Giordan *et al.*, 2022; Jay, 2022; Meng *et al.*, 2022). Several methods for tsunami hazard analysis and evacuation planning have been introduced, such (i) as probabilistic tsunami hazard assessment (PTHA), (ii)

deterministic tsunami hazard assessment (DTHA), (iii) geophysical-seismic analysis, (iv) sedimentary tsunami deposits, and (v) historical records (Haider *et al.*, 2023; Ibrahim *et al.*, 2023), as well as network analysis (Das *et al.*, 2024). These methods utilise GIS and remote sensing to ensure reproducible analysis across space and time.

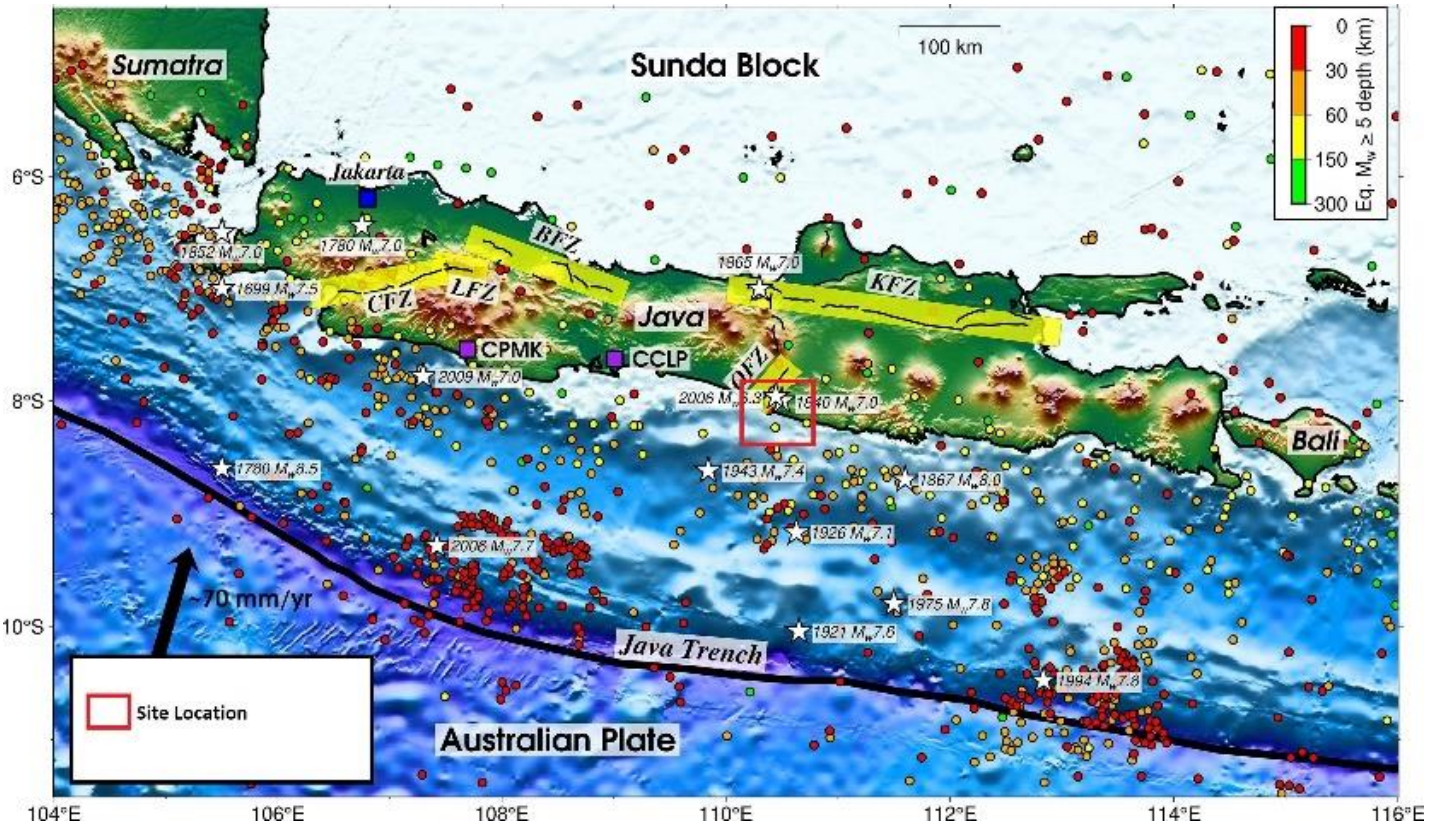

Source: Pusat Sumber dan Bahaya Gempa Indonesia (modified Pusgen, 2017).

Figure 1. Distribution of Earthquake Epicentre Points and Seismic Gaps in the Southern Island of Java.

However, most of these methods are only partially applicable to the coastal areas of Indonesia for several reasons, including the lack of detailed base maps and complete historical data. Therefore, this research utilises Landsat 8 OLI satellite imagery and the ALOS PALSAR DEM. Both datasets were employed to extract information in the form of land use and slope, which were used to visualise the potential hazards in the study area using the Berryman (2006) method. Geospatial researchers widely use Berryman's model because it is relatively easy to apply ; however, it does not account for tsunami source and propagation factors (Berryman, 2006; Fuentes *et al.*, 2021).

Another non-structural mitigation measure is the construction of tsunami evacuation routes (Oetjen *et al.*, 2022). The evacuation route should be the most effective route from danger to safety. Using the GIS analysis, effective evacuation routes can be created with a network analyst (Deliry & Uyguçgil, 2023). Within the network analysis, the closest facility feature indicates the optimal path from one point to another. Additionally, evacuation routes were planned by considering the inundation modelling produced during tsunami hazard map development (Karpouza *et al.*, 2023). Safe points for tsunami evacuation were selected by overlaying the land-use map on a tsunami inundation map. The results from the network analysis were then visualised as an informative map to facilitate readers' understanding of the content.

2. Research Methods

The research site is a combination of the coastal areas of the Opak and Progo watersheds, covering an area of 153.4 km^2. This region includes parts of the Kulon Progo, Bantul, and Gunung Kidul Regencies. A coastal region map of the Opak-Progo watershed is shown in Figure 2.

The datasets used in this study included Landsat 8 OLI satellite images, ALOS PALSAR, DEM images, and shapefiles of the Opak and Progo watersheds, road networks, and coastlines. The research method was divided into two parts: tsunami hazard analysis using the Berryman method and evacuation route planning using network analysis.

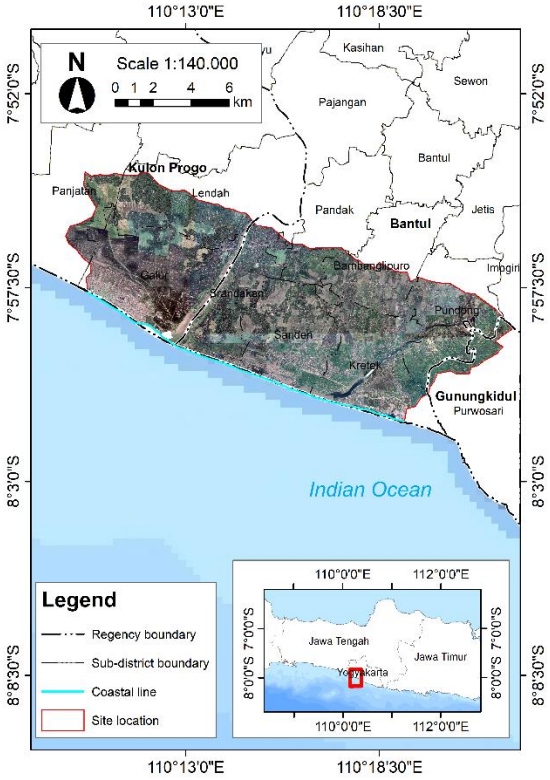

Figure 2. Site Location.

2.1. Tsunami Hazard Analysis

The tsunami hazard analysis was conducted using the numerical formulation method developed by Berryman (2006). This numerical calculation is presented in Equation 1:

$$Hloss = (167n\,2 / H0\,1/3) + 5\,Sin\,S \quad (1)$$

In this equation, the variable *n* represents the surface roughness coefficient derived from land use interpretation. The land-use interpretation was performed on the Landsat 8 OLI images through visualisation. This study used Level 1 Landsat 8 imagery from the year 2023. Each land use type has a different surface roughness coefficient; the higher the coefficient, the more complex the land use is for waterlogging, and vice versa. The surface roughness coefficient values for each land-use type are listed in Table 1. The H_0 variable denotes the wave height when the wave reaches the land, with a height of 3 m used in this study. The S variable represents the slope value obtained from the derivation of ALOS PALSAR DEM data, expressed in degrees radians (Figure 4).

Table 1. Coefficient of surface roughness.

Land use	Coefficient of surface roughness
Waterbody	0.007
Swamp	0.015
Pond	0.010
Sand	0.018
Shrubs	0.040
Grassland	0.020
Forest	0.070
Plantation	0.035
Agricultural field	0.030
Rice field	0.020
Cropland	0.025
Settlement/build-up area	0.050
Mangrove	0.060
Open land	0.015

Source: BNPB, 2023.

The results of the Hloss calculations were then used to calculate the cost distance, which determined the estimated inundation area, incorporating shoreline data. This cost distance produced a hazard index, which was subsequently utilised with a fuzzy logic approach as input data for hazard classification. In this approach, the greater the hazard index value, the closer the fuzzy graduated class value will be to one (high-hazard class); conversely, a value closer to zero indicates a low-hazard class. The fuzzy logic approach resulted in three tsunami hazard classes : low, medium, and high.

2.2. Tsunami Evacuation Route Planning

Evacuation route planning was conducted using GIS and network analyses. The closest facilityfeature was employed to determine the optimal route from an incident point to a facility point. In this case, the incident points are located in high-hazard zones, tourist attractions, or densely populated residential areas. Facility points, in contrast, are designated evacuation points located in low-hazard zones.

3. Results and Discussion

3.1. Tsunami Hazard Level

Using Berryman's method (2006), tsunami hazard maps were generated based on parameters such as the surface roughness coefficient, slope, coastline, and wave height scenarios upon reaching land. The surface roughness coefficient was derived from land-use information in the study area and interpreted visually using Landsat 8 OLI imagery. This study utilized Level 1 Landsat 8 imagery from the year 2023. The dominant land uses in the study area included rice fields and settlement/built-up areas. Of the 153.4 km² study area, rice fields accounted for 61.2 km² (39.9%), while settlement/built-up areas covered 54.4 km² (35.5%). A land-use accuracy test was conducted at 20 sampling locations, with results compiled into a configuration table. The overall accuracy of the interpretation was 81%. This error was attributed to the interpreter's difficulty in identifying land use and the necessity of local knowledge of the study area. Additionally, the uneven distribution and number of samples may have affected accuracy. The results of the land-use interpretation at these research sites are presented in Figure 3.

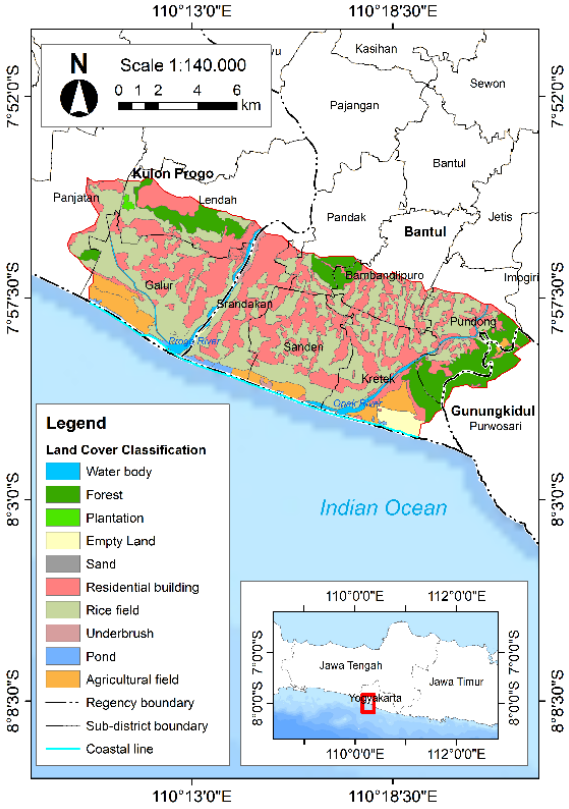

Figure 3. Land Use Classification.

The slope was derived from ALOS PALSAR DEM data and classified into four slope categories: smooth, wavy, steep, and very steep (Setiawan *et al.*, 2018). As shown in Figure 4, fine-grade slopes predominated in the research location, primarily due to its positioning in the southern-coastal area of mainland Java, where the relief tends toward smoother slopes.

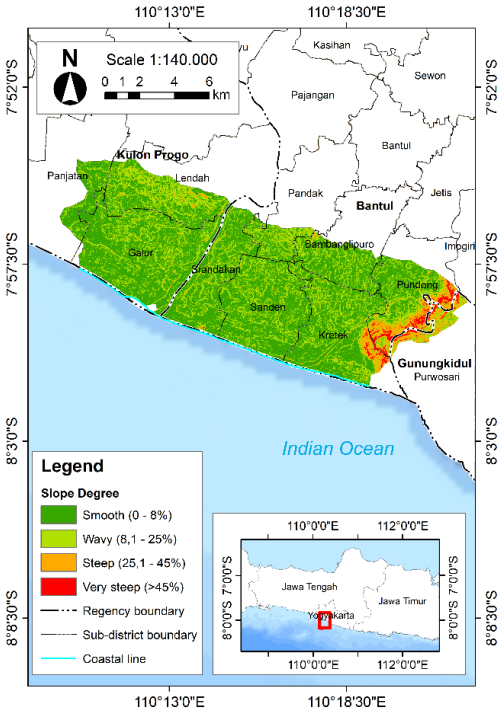

Figure 4. Slope Classification.

However, the eastern area of the Opak Watershed exhibited steep to very steep reliefs, which can minimize the potential for inundation caused by tsunami waves. Previous research has shown that undulating, hilly, and steep geomorphological conditions can reduce tsunami wave impacts (Lynett, 2011; Rikumahu, 2024).

Combining the parameters of surface roughness coefficient, slope, coastline, and a wave height scenario of 3 m resulted in the tsunami hazard map shown in Figure 5. Three hazard classes were identified: low, medium, and high. High-hazard areas accounted for 89.2 km² (58.1%) of the total area, medium-hazard areas for 26.7 km² (17.4%), and low-hazard areas for 37.5 km² (24.5%).

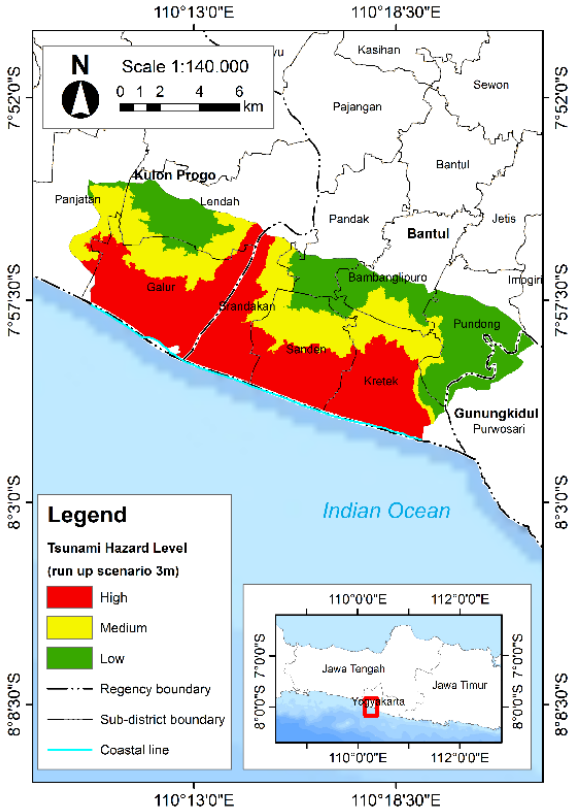

Figure 5. Tsunami Hazard Level.

The villages affected by the tsunami are presented in in Table 2.

Table 2. The villages affected by the tsunami.

Sub-district	Village
Panjatan	Panjatan
	Krembengan
	Cerme
	Kanoman
	Bugel
Lendah	Bumirejo
	Wahyuharjo
	Jatirejo
	Sidorejo
Galur	Karangsewu
	Banaran
	Kranggan
	Nomporejo
	Brosot
	Pandowan
	Tirtorahayu
Srandakan	Trimurti
	Poncosari
Sanden	Gadingsari
	Murtigading
	Gadingharjo
	Srigading
Kretek	Tirtosari
	Parangtritis
	Donotirto
	Tirtomulyo
	Tirtoharjo
Pandak	Caturharjo
	Tirtoharjo
	Gilangharjo
Bambanglipuro	Sidomulyo
	Mulyodadi
Purwosari	Seloharjo
	Panjangrejo
	Srihardono
Purwosari	Girijati
	Giriasih
	Giritirto

High-hazard class areas were located near coastlines and watersheds, characterized by gentle slopes and land uses with low surface roughness, such as paddy fields and ponds. Areas classified as medium hazard were predominantly occupied by settlements/buildings, with higher slope conditions and situated further from rivers and coastlines. Low-hazard zones comprised steeper slopes and were the farthest from the coastline and rivers, with forests dominating land use. Previous studies have shown that temporal changes in tsunami risk due to land-use changes and coastal population growth have been highlighted as key factors influencing tsunami vulnerability and risk assessment (Hou *et al.*, 2023). The visualisation indicates that river flow patterns also affect tsunami hazard levels. Prior research has shown that river flow patterns affect the flow depth and arrival time of tsunami hazards(Zamora *et al.*, 2021).

The Progo River has a straighter flow than the Opak River; therefore, when a tsunami occurs,waves can more easily enter a straight river compared to a meandering one. That is why the area around the Progo River has a higher hazard level than that around the Opak River. Additionally, the topographic differences between the two watersheds contribute to the Opak watershed's lower hazard classification. The Opak Watershed's steeper topographic characteristics result from its location in an active fault area, namely the Opak fault. Previous research suggests that topographicfactors in coastal areas influence tsunami inundation (Pattiaratchi, 2020). Therefore, rock movement occurs more frequently in this area than in the Progo watershed. The results of this hazard modelling show that land use and slope, which represent surface morphology, significantly influence tsunamigenic hazards in the region. Previous research has suggested that factors such as land use, slope, and surface morphology play crucial roles in determining tsunami hazards (Ramalho *et al.*, 2024).

3.2. Tsunami Evacuation Route Planning

Selecting safe points is crucial for developing evacuation routes in coastal areas. Various factors must be considered to ensure the effectiveness of evacuation plans. Factors such as population density, depth of danger zone, individual walking speed, and uncertainty of future tsunami events play an important role in determining safe evacuation areas. However, this study focused on the distance from the coastline, river mouths, river bodies, and industrial areas. The points used as evacuation sites are indicated in green. The evacuation points, from west to east, include Muhammadiyah 1 Pundong Junior High School Field, N 1 Galur High School Field, N 1 Sanden High School Field, and Panggang 3 State Elementary School Field.

The starting points used to create evacuation routes were located in high inundation zones and areas with high human activity, such as tourist spots and densely populated settlements. The starting points, from west to east, include Trisik Beach, Baru Beach, Kuwaru Beach, Goa Cemara Beach, Samas Beach, Depok Beach, and Gumuk Pasir Tourism. Using the identified danger and safety points, network analysis was performed employing the closest facility method, resulting in an evacuation route depicted in Figure 6.

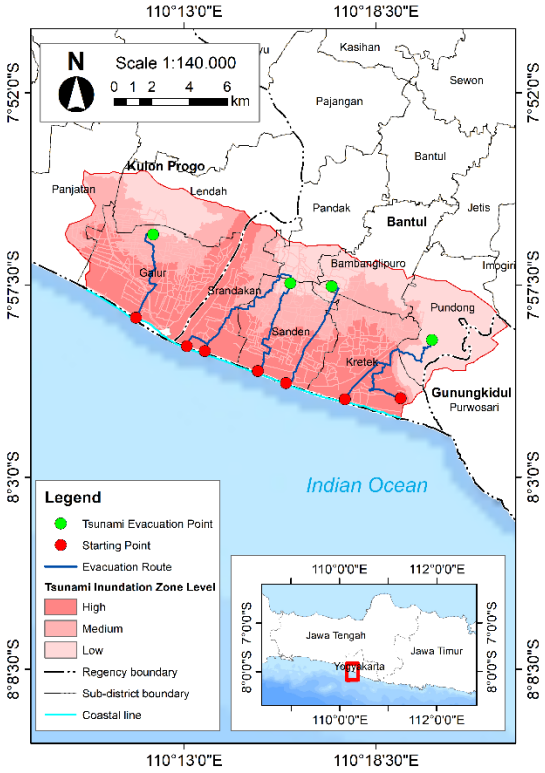

Figure 6. Planning Tsunami Evacuation Routes in the Coastal Areas of the Opak-Progo Watersheds.

The closest facility analysis also considered bridge aspects due to their high risk. Bridges were treated as point barriers; thus, the analysis avoided routing through these points. Six main tsunami evacuation routes were identified. These routes are aligned vertically with the coastline and lead directly to the designated evacuation locations. Consequently, the results of this network analysis require improvement. First, the evacuation routes presented are designed for motorised vehicles, and thus, do not account for the capacity of the evacuation routes.

However, this study incorporates pedestrian-friendly evacuation routes, as they enhance the effectiveness and safety of overall evacuation in tsunami-prone areas. This approach aligns with previous studies that used multicriteria-based Least Cost Path Analysis for pedestrian and vehicle scenarios, where pedestrian scenarios were considered more realistic due to their proximity to the road network accommodating both pedestrians and vehicles (Jati *et al.*, 2023). The study underscores the importance of considering both pedestrian-friendly routes and vehicle options.

4. Conclusion

Geovisualisation of tsunami hazards under a 3-meter run-up height on the Opak-Progo coast resulted in three tsunami hazard classes: low, medium, and high. High-hazard class areas cover 89.2 km (58.1% of the total area), medium-hazard class areas cover 26.7 km (17.4%), and low-hazard class areas cover 37.5 km (24.5%) of the total study area. The evacuation route analysis identified

six routes, aligned with the coastline, leading to four evacuation points: the fields of 213 SMP Muhammadiyah 1 Pundong, SMA N 1 Galur, SMA N 1 Sanden, and SD Negeri 3 Panggang. These findings are crucial for updating spatial planning and enhancing both structural and and nonstructural mitigation, including evacuation plans, routes, and community preparedness. A limitation of this study is the lack of field validation; thus, recommendations for evacuation site capacity need revision. Future research should include field survey validation.

Acknowledgements

This research was supported by, the Faculty of Geography, Gadjah Mada University. The authors acknowledge the reviewers for their constructive feedback and suggestions for future research.

Author Contributions

Conceptualization: Sudaryatno, S., Sumantyo, J. T. S., & Purwanto, T. H.; **methodology**: Sudaryatno, S., Akbar, M. F. A., Gita, A. R., & Shalih, O.; **investigation**: Sudaryatno, S., Akbar, M. F. A.; **writing—original draft preparation**: Sudaryatno, S., Akbar, M. F. A., Gita, A. R., & Shalih, O.; **writing—review and editing**: Sudaryatno, S., & Shalih, O.; **visualization**: Sudaryatno, S., Akbar, M. F. A., & Gita, A. R. All authors have read and agreed to the published version of the manuscript.

Conflict of interest

All authors declare that they have no conflicts of interest.

Data availability

Data is available upon Request.

Funding

This research received no external funding.

References

Adityawan, M. B., & Tanaka, H. (2016). Investigating the 2011 Tsunami Impact on the Teizan Canal and the Old Ri-ver Mouth in Sendai Coast. *Springer Link*, 125–136. doi: 10.1007/978-3-319-28528-3_9

Amalia Listiani, & Fuji Lestari. (2023). Tsunami Potential Prediction with Artificial Neural Network. *International Journal of Scientific Research in Science, Engineering and Technology*, 231–236. Doi: 10.32628/IJSRSET2310130

Andriani, A., Adji, B. M., & Ramadhani, S. (2023). The Analysis of Impact and Mitigation of Landslides Using Analytical Hierarchy Process (AHP) Method. *Springer Link*, 457–466. doi: 10.1007/978-981-16-9348-9_40

Bai, Y., Yamazaki, Y., & Cheung, K. F. (2023). Intercomparison of hydrostatic and nonhydrostatic modeling for tsu-nami inundation mapping. *Physics of Fluids*, 35(7). doi: 10.1063/5.0152104

Berryman, K. (2006). *Review of Tsunami Hazard and Risk in New Zealand*. Retrived from https://www.hbemergency.govt.nz/assets/Documents/Hazard-Reference-Documents/review-of-tsunami-hazard-and-risks-in-nz-sept-05.pdf

BNPB. (2023). *RBI RISIKO BENCANA INDONESIA BNPB "Memahami Risiko Sistemik di Indonesia"*. Retrived from https://perpustakaan.bnpb.go.id/bulian/index.php?p=show_detail&id=2063

Bosma, C., Shumlich, A., Rankin, M., Kouhi, S., & Amouzgar, R. (2023). Integrating Topographic and Bathymetric Data for High-Resolution Digital Elevation Modeling to Support Tsunami Hazard Mapping. *Oceanography*, 36(1), 72-73. doi: 10.5670/oceanog.2023.s1.23

Das, S., Baral, A., Rafizul, I. M., & Berner, S. (2024). Efficiency enhancement in waste management through GIS-based route optimization. *Cleaner Engineering and Technology*, 21, 100775. doi: 10.1016/j.clet.2024.100775

Deliry, S. I., & Uyguçgil, H. (2023). Accessibility assessment of urban public services using GIS-based network analysis: a case study in Eskişehir, Türkiye. *GeoJournal*, 88(5), 4805–4825. doi: 10.1007/s10708-023-10900-y

Ehara, A., Salmanidou, D. M., Heidarzadeh, M., & Guillas, S. (2023). Multi-level emulation of tsunami simulations over Cilacap, South Java, Indonesia. *Computational Geosciences*, 27(1), 127–142. doi: 10.1007/s10596-022-10183-1

Friska, V., Arisa, D., Marzuki, M., & Monica, F. (2022). Indo-Australian Plate Velocity Measurement During Interseismic Phase in 2010–2014 Using Sumatran GPS Array (SuGAr) Data. *Springer Link*, 925–934. doi: 10.1007/978-981-19-0308-3_73

Fuad, M. A. Z., Hardiansyah, F., & Semedi, B. (2022). Analysis of Coastline Changes in Palu Bay, Central Sulawesi after the 2018 Tsunami Based on Sentinel 1 Satellite Imagery Using the Digital Shoreline Analysis System (DSAS) Method. *Jurnal Perikanan Dan Kelautan*, 27(3), 304. doi: 10.31258/jpk.27.3.304-312

Fuentes, M., Uribe, F., Riquelme, S., & Campos, J. (2021). Analytical Model for Tsunami Propagation Including Source Kinematics. *Pure and Applied Geophysics*, 178(12), 5001–5015. doi: 10.1007/s00024-020-02528-7

Giordan, D., Luzi, G., Monserrat, O., & Dematteis, N. (2022). Remote Sensing Analysis of Geologic Hazards. *Remote Sensing*, 14(19), 4818. doi: 10.3390/rs14194818

Haider, R., Ali, S., Hoffmann, G., & Reicherter, K. (2023). A multi-proxy approach to assess tsunami hazard with a preliminary risk assessment: A case study of the Makran Coast, Pakistan. *Marine Geology*, 459, 107032. doi: 10.1016/j.margeo.2023.107032

Hartoko, A., Helmi, M., & Sukarno, M. (2016). Spatial Tsunami Wave Modelling For The South Java Coastal Area, Indonesia. *International Journal of GEOMATE*, 11(25), 2455-2460.

Herlianto, M. (2023). Early Disaster Recovery Strategy: The Missing Link in Post-Disaster Implementation in Indonesia. *Influence: International Journal Of Science Review*, 5(2), 80–91. doi: 10.54783/influencejournal.v5i2.138

Hou, J., Gao, Y., Fan, T., Wang, P., Wang, Y., Wang, J., & Lu, W. (2023). Tsunami Risk Change Analysis for Qidong County of China Based on Land Use Classification. *Journal of Marine Science and Engineering*, 11(2), 379. doi: 10.3390/jmse11020379

Ibrahim, Syamsidik, Azmeri, Hasan, M., Irwansyah, A., & Al Farizi, M. D. (2023). Assessing tsunami vertical evacuation processes based on probabilistic tsunami hazard assessment for west coast of Aceh Besar, Indonesia. *Geoenvironmental Disasters*, 10(1), 8. doi: 10.1186/s40677-023-00238-5

Jati, B. A. E. K., Akbar, M. F. Al, Wahyuni, T., Khasanah, E. U., Paramanandi, A. R. G., Sutiono, H. E. C. P., Setyaningsih, D. P., Widyatmanti, W., & Wibowo, T. W. (2023). Analysis Of Tsunami Evacuation Route Planning In Kulon Progo Regency. *International Journal of Remote Sensing and Earth Sciences (IJReSES)*, 20(1), 16. doi: 10.30536/j.ijreses.2023.v20.a3823

Jay, G. (2022). Remote Sensing of Natural Hazards (B. Ahmed & A. Alam, Eds.). *MDPI Remote Sensing*, 12, 3363. doi: 10.3390/books978-3-0365-4307-9

Karpouza, M., Bathrellos, G. D., Kaviris, G., Antonarakou, A., & Skilodimou, H. D. (2023). How could students be safe during flood and tsunami events?. *International Journal of Disaster Risk Reduction*, 95, 103830. doi: 10.1016/j.ijdrr.2023.103830

Katsumata, A., Tanaka, M., & Nishimiya, T. (2021). Rapid estimation of tsunami earthquake magnitudes at local distance. *Earth, Planets and Space*, 73(1), 72. doi: 10.1186/s40623-021-01391-7

Kirana, A., & Bature, S. S. (2022). Socialization of Natural Disaster Mitigation to Minimize the Impact of the Risk of Economic Loss in the Citarum River Basin (DAS) West Bandung Regency. *International Journal of Research in Community Services*, 3(4), 120–126. doi: 10.46336/ijrcs.v3i4.339

Liu, J., Brunner, P., & Tokunaga, T. (2022). *Modeling seawater flooding, ponding, and infiltration processes under future tsunami scenarios: A case study at Niijima Island, Japan*. Retrived from https://doi.org/10.5194/egusphere-egu22-4643

Lynett, P. J. (2011). Tsunami Inundation, Modeling of. In Extreme Environmental Events. *Springer New York*, 1008–1021. doi: 10.1007/978-1-4419-7695-6_53

Meng, F., Jia, C., Wang, X., Gao, F., Liu, J., Shao, M., & Dong, H. (2022). The Development History of Geological Hazard Investigation Work Based on Remote Sensing Technology : - Taking Shandong Province as an Example. *International Conference on Geology, Mapping and Remote Sensing (ICGMRS)*, 922–925. doi: 10.1109/ICGMRS55602.2022.9849270

Muttaqy, F., Nugraha, A. D., Mori, J., Puspito, N. T., Supendi, P., & Rohadi, S. (2022). *Seismic Imaging of Lithospheric Structure Beneath Central-East Java Region, Indonesia: Relation to Recent Earthquakes*. Retrived from https://doi.org/10.3389/feart.2022.756806

Oetjen, J., Sundar, V., Venkatachalam, S., Reicherter, K., Engel, M., Schüttrumpf, H., & Sannasiraj, S. A. (2022). A comprehensive review on structural tsunami countermeasures. *Natural Hazards*, 113(3), 1419–1449. doi: 10.1007/s11069-022-05367-y

Ovando, P. (2023). Watershed. In Dictionary of Ecological Economics. *Edward Elgar Publishing*, 584–584. doi: 10.4337/9781788974912.W.12

Pattiaratchi, C. (2020). Influence of Ocean Topography on Tsunami Propagation in Western Australia. *Journal of Marine Science and Engineering*, 8(9), 629. doi: 10.3390/jmse8090629

Ramalho, I., Omira, R., & Kim, J. (2024). *Effect of volcanic islands offshore morphology on the tsunami generation and hazard extent from coastal cliff-failures*. Retrived from https://doi.org/10.5194/egusphere-egu24-19584

Richard, G. L., Msheik, K., & Duran, A. (2023). A preliminary depth-integrated model for tsunamis propagation including water compressibility and seafloor elasticity. *European Journal of Mechanics - B/Fluids*, 99, 84–97. doi: 10.1016/j.euromechflu.2023.01.004

Rikumahu, V. D. (2024). Tsunami Vulnerability Mapping of Coastal Areas to Confront the Banda Detachment Tsu-nami (Case Study at Tual City). *EGUsphere*, 1–13. doi: 10.5194/egusphere-2023-3021

Rusydi, A. N., & Masitoh, F. (2023). Identification of Sea Surface Temperature Anomaly during Earthquake in Sou-thern Java Island using Google Earth Engine Datasets. *Indonesian Journal of Geography*, 55(1), 69. doi: 10.22146/ijg.68247

Ry, R. V., Cummins, P. R., Hejrani, B., & Widiyantoro, S. (2023). 3-D shallow shear velocity structure of the Jakarta Basin from transdimensional ambient noise tomography. *Geophysical Journal International*, 234(3), 1916–1932. doi: 10.1093/gji/ggad176

Setiawan, B., Yudono, P., Waluyo, S., Studi Agronomi, P., Pertanian, F., & Gadjah Mada, U. (2018). Evaluation of the Agricultural Land Utilization Types for Mitigation of Land Degradation in Giritirta, Pejawaran, Banjarnegara. *Vegetalika*, 7(2), 1-15.

Shalih, O., Setiadi, H., Nurlambang, T., & Sumadio, W. (2020). Toward a community resilience framework for disaster risk management. a case study: Landslide Cisolok in Sukabumi 2018 and Sunda strait tsunami in Pandeglang 2018. *E3S Web of Conferences*, 156. doi: 10.1051/e3sconf/202015601011

Sinaga, R., & Ronoatmojo, I. S. (2022). Analysis Of Earthquake-Prone Areas For Disaster Mitigation In The Sumatra Trench And Surroundings. *Journal of Geoscience Engineering & Energy*, 108–115. doi: 10.25105/jogee.v3i1.12998

Srinivasa Kumar, T., Pattabhi Rama Rao, E., Patanjali Kumar, Ch., Manneela, S., Ajay Kumar, B., Saikia, D., Mahen-dra, R. S., Murty, P. L. N., & Padmanabham, J. (2023). Tsunami Early Warning Services. In Social and Econo-mic Impact of Earth Sciences. *Springer Nature Singapore*, 351–375. doi: 10.1007/978-981-19-6929-4_18

Sudaryatno, S., Sumantyo, J. T. S., Purwanto, T. H., Hidayat, I. R., & Nasikha, M. A. (2022). Simulated Mitigation of Tsunami Disasters in the Coastal Area of Purworejo Regency, Central Java, Indonesia. *Forum Geografi*, 36(1), 54-65. doi: 10.23917/forgeo.v36i1.16984

Sugawara, D. (2020). Trigger mechanisms and hydrodynamics of tsunamis. In Geological Records of Tsunamis and Other Extreme Waves. *Elsevier*, 47–73. doi: 10.1016/B978-0-12-815686-5.00004-3

Tanaka, H., & Tinh, N. X. (2022). Tsunami Propagation Into Rivers In Tohoku Area During The 2022 Tonga Volcano-Tsunami. *Journal of Japan Society of Civil Engineers*, 78(2), 151-156. doi: 10.2208/kaigan.78.2_I_151

Tarigan, T., Subardjo, P., Jurusan, D. N., Kelautan, I., Perikanan, F., Diponegoro, U., Soedarto, J. H., & Semarang, T. (2015). *Analisa Spasial Kerawanan Bencana Tsunami Di Wilayah Pesisir Kabupaten Kulon Progodaerah Istimewa Yogyakarta*. Retrived from: http://ejournal-s1.undip.ac.id/index.php/jose.50275Telp/fax

Wang, Y., Wang, P., Kong, H., & Wong, C.-S. (2022). Tsunamis in Lingding Bay, China, caused by the 2022 Tonga volcanic eruption. *Geophysical Journal International*, 232(3), 2175–2185. doi: 10.1093/gji/ggac291

Widiyantoro, S., Gunawan, E., Muhari, A., Rawlinson, N., Mori, J., Hanifa, N. R., Susilo, S., Supendi, P., Shiddiqi, H. A., Nugraha, A. D., & Putra, H. E. (2020). Implications for megathrust earthquakes and tsunamis from seismic gaps south of Java Indonesia. *Scientific Reports*, 10(1), 15274. doi: 10.1038/s41598-020-72142-z

Zamora, N., Catalán, P. A., Gubler, A., & Carvajal, M. (2021). Microzoning Tsunami Hazard by Combining Flow Depths and Arrival Times. *Frontiers in Earth Science*, 8. doi: 10.3389/feart.2020.591514

Zelaya, C., Olivares, I., Pulgar, N., & Henríquez, C. (2023). Tsunami inundation chart (CITSU) as a tool to support coastal area management: a case study for Coronel. *Revista Geográfica de Chile Terra Australis*, 2(2). doi: 10.23854/07199562.202258esp.Zelaya35

Zorn, E. U., Orynbaikyzy, A., Plank, S., Babeyko, A., Darmawan, H., Robbany, I. F., & Walter, T. R. (2022). Identification and ranking of subaerial volcanic tsunami hazard sources in Southeast Asia. *Natural Hazards and Earth System Sciences*, 22(9), 3083–3104. doi: 10.5194/nhess-22-3083-2022